Liquid Crystals
Publication details, including instructions for authors and subscription information:
http://www.informaworld.com/smpp/title~content=t713926090

Remarks on the geometry of micelles, bilayers and cell membranes

Y. Bouligand

Online publication date: 06 August 2010

To cite this Article Bouligand, Y.(1999) 'Remarks on the geometry of micelles, bilayers and cell membranes', Liquid Crystals, 26: 4, 501 — 515
To link to this Article: DOI: 10.1080/026782999204949
URL: http://dx.doi.org/10.1080/026782999204949

LIQUID CRYSTALS, 1999, VOL. 26, NO. 4, 501–515

Remarks on the geometry of micelles, bilayers and cell membranes

Y. BOULIGAND*

Histo- et Cyto-physique, EPHE, Laboratorie Arago, F-66650 Banyuls-sur-mer, France

(*Received 10 September 1998; accepted 16 October 1998*)

Starting from simple geometric properties of parallel surfaces, it is suggested that bilayers, and also monolayers, present two spontaneous principal curvatures γ and γ', so that a narrow disc of freely deformable bilayer might adopt either a 'saddle' shape, or a 'hat' shape, or a cylindrical shape. Besides the usually considered spontaneous splay $c_0 = \gamma + \gamma'$, there is also a spontaneous gaussian curvature $g_0 = \gamma\gamma'$, with noticeable effects in strongly curved bilayers. An excess of area of the median hydrophobic level with respect to the mean area occupied by the two hydrophilic layers creates a saddle shape, whereas a deficit leads to a hat shape, the equality corresponding to a cylindrical shape. The usual two layers theory of the spontaneous curvature seems to be improved by considering the role of a median layer. We have tried to illustrate this new point of view by many examples. Due to their asymmetry, monolayers and cell membranes give rise to micelles and vesicles of comparable geometries, but of very different sizes. At the considered scales, a term of order higher than quadratic, such as $k_t(cc' - \gamma\gamma')^2$, seems to be necessary in the expression of the elastic energy.

1. Introduction

Amphiphilic compounds assemble into diverse types of aggregates: *spherical* micelles, *elongated* micelles, *branched* micelles, *flat* or *discoidal* micelles, indefinite *cylindrical* micelles (linear or branched), *ribbons*, indefinite *bilayers*, etc. These micelles or bilayers also arrange themselves into more or less ordered systems, corresponding to different mesophases. The origin of these shapes can be understood through different approaches: the shapes of the molecules themselves, their motions and interactions, depending on chemical and physical environment, the elastic energies and also geometrical considerations, that we hope to develop here.

Among the first theories of lyotropic aggregates, one is due to Winsor [1] who considered the cohesive energies of the different molecules and chemical groups interacting at an interface, introducing a parameter R to which a connection to curvature can be established (review in [2]). One has R = 1 in bilayers, whereas R > 1 corresponds to a divergence of lipophilic extremities and R < 1 to a divergence of hydrophilic extremities. Similar ideas were developed by Tanford [3] and Israelachvili and coworkers [4], indicating the importance of the ratio V/AR, V being the volume of an amphiphilic molecule, A the area occupied by this molecule at the outer surface of the micelle, and R a radius corresponding to the distance scanned by the molecule from the outer surface to the centre of a spherical micelle (R_S), or to the axis of a cylindrical micelle (R_C) or to the median level of a flat micelle or a bilayer (R_B). This ratio V/AR is 1/3 in a spherical micelle, 1/2 in a cylindrical one and 1 in a planar bilayer. V is constant but not A; the assumption of A constant would give $R_S/3 = R_C/2 = R_B = V/A$, but A depends on the chemical environment and more simply, one has $R_S > R_C > R_B$, with generally less important differences between the three radii, as will be seen below. Several articles use similar parameters or more complex ones, in association with calculations of elastic energies [5–7].

We propose to consider a short series of geometrical parameters of the same type: length, area, volume, radii of curvature, directly accessible (or less directly), whose association allows one to discuss the expected shapes of molecular aggregates and bilayers present in lyotropic preparations.

2. Shape similarity of lyotropic units and cell organelles

The shapes of micelles are mainly known from the study of mesophases in which they associate and among these shapes there are those recalled above: spheres, cylinders (branched or not), surfaces (toroidal or not). These micellar shapes are reproduced in vesicles (also

*Present address: EPHE and IBT, 10 rue A.-Bocquel, F-49100 Angers, France.

Journal of Liquid Crystals ISSN 0267-8292 print/ISSN 1366-5855 online
http://www.tandf.co.uk/JNLS/lct.htm
http://www.taylorandfrancis.com/JNLS/lct.htm

artificial vesicles), tubes and more complex systems of membranes or bilayers in the cytoplasm of living cells, with dimensions compared with those of micelles being multiplied by a variable factor, often close to 10, but actually varying from 3 to 10^4. These shapes are therefore directly accessible by transmission electron microscopy or in rare cases by light microscopy. We illustrated this fact some years ago in a paper entitled *Geometry and topology of cell membranes*, with main examples and literature sources [8(*a*, *b*)] and we shall see below some new examples. In the present work, we give the reasons for this similarity of shapes observed on two different scales, and we also indicate that many patterns known in cytoplasmic organelles might have their counterpart in micellar structures and lyotropic mesophases; they are not usually considered, since they are difficult to deduce from X-ray diffraction diagrams.

3. Parallel equidistant surfaces

Let us return to a classical representation of parallel surfaces (figure 1), as in optics handbooks, for the definition of caustics. Consider a smooth surface Σ_0 and its parallel surface Σ, whose normals form a family of straight lines, tangent to two *focal surfaces* or *caustics* σ and σ'. A system of curvilinear coordinates u, u' can be defined along the lines of principal curvature, and along the normals to these parallel surfaces, with a third (non-curvilinear) coordinate e.

An element of area $dS_0 = du_0\, du_0'$, a small curvilinear rectangle, centred in M_0 on Σ_0, corresponds on Σ to a homologous element of area $dS = du\, du'$, centred in M. There are two centres of curvature C and C' on the normal to S_0 in M_0, whose coordinates are respectively $(0, 0, -R)$ and $(0, 0, -R')$. This is represented in figure 1, where Σ_0 is chosen with a positive gaussian curvature $(RR')^{-1}$. This gaussian curvature is negative for all surfaces Σ cutting the segment CC', the points C and C' excepted, and is positive outside of CC' along the normal in M_0. The area dS presents similar sign changes along this normal, being negative between C and C' and positive outside. More precisely, if $\mathbf{n}$ is a unit vector along the normal in M_0, one has

$$\mathbf{CM}_0 = R\mathbf{n}, \qquad \mathbf{C'M}_0 = R'\mathbf{n}.$$

Let us compare dS in $M(0, 0, e)$ to dS_0 in $M_0(0, 0, 0)$:

$$du/du_0 = \mathbf{CM}/\mathbf{CM}_0 = (\mathbf{CM}_0 + \mathbf{M}_0\mathbf{M})/\mathbf{CM}_0 = (R + e)/R.$$

Similarly, $du'/du_0' = (R' + e)/R'$ and therefore:

$$dS/dS_0 = (du\, du')/(du_0\, du_0') = (R + e)(R' + e)(RR')^{-1}.$$

If $c = R^{-1}$ and $c' = R'^{-1}$ are the principal curvatures, one finds:

$$dS/dS_0 = A(e) = 1 + e(c + c') + e^2 cc' \qquad (1)$$

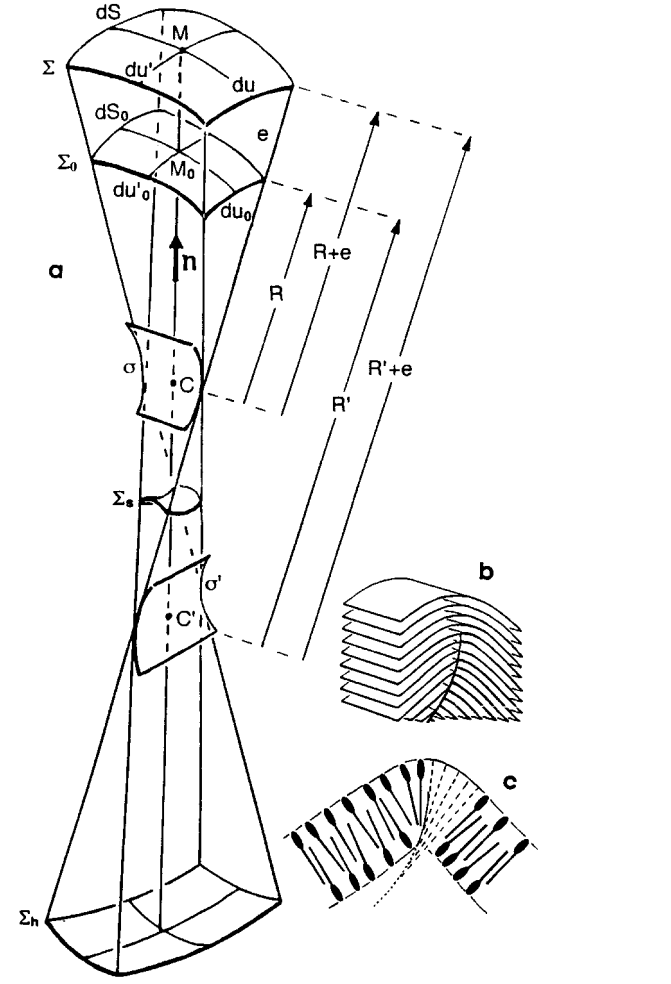

Figure 1. (*a*) Set of parallel surfaces, hat-shaped in Σ_0, Σ and Σ_h, or saddle-shaped in Σ_s, with their caustics σ and σ', their curvature centres C and C', their radii R and R' of principal curvature of surface Σ_0, and the constant distance e separating Σ from Σ_0. The area dS or dS_0 of curvilinear rectangles of sides du, du' or du_0, du_0', considered along the lines of principal curvature. (*b*) Stack of parallel and equidistant surfaces, which are cylindrical and seen in cross-section, showing a discontinuity corresponding to a caustic seen in cross-section, but such walls are absent in smectics. (*c*) The presence of a caustic within a bilayer would create a severe disturbance; normals to bilayer are indicated by dashed lines touching tangentially the caustic and, within this domain of high curvature, molecules cannot arrange without modifying the bilayer thickness. Such situations are relaxed in general by a smoother distribution of curvatures.

which indicates that $A(e)$ varies as dS, since dS_0 is constant and chosen positive. $A(e)$ is represented by a parabola in figure 2, cutting the axis e at two points of abcissa $-R$ and $-R'$, since $A(-R) = A(-R') = 0$.

4. Hat-shaped and saddle-shaped bilayers

A bilayer can be schematized by three parallel surfaces cutting the normal axis e at points M_1, M_2, M_3 of

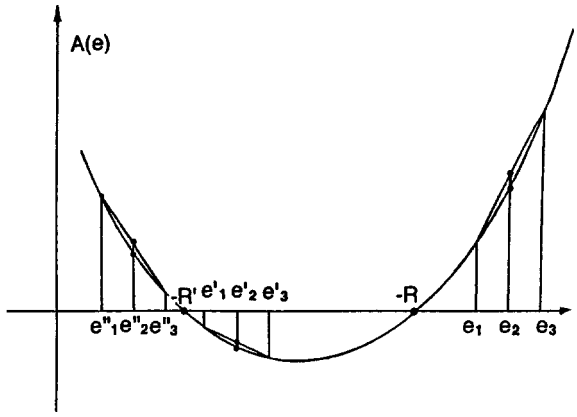

Figure 2. Representation of variations of $A(e) = dS(e)/dS(0)$; see the text.

coordinates e_1, e_2, e_3, so that $e_2 = (e_1 + e_3)/2$ (figure 2). The three points M_1, M_2, M_3 are grouped either between C and C' or outside, on the right or on the left along the e axis, but the intermediate situations are forbidden, since the centres C and C' and the caustics σ and σ' themselves would lie within the bilayer, creating discontinuities, as was shown in earlier work [8(*c*, *d*)] and as can be seen in figure 1(*b*, *c*).

When M_1, M_2, M_3 lie outside of CC' (figure 1), the parallel surfaces are locally elliptical and the bilayer is *hat-shaped*, a term adopted in [6(*b*)]. In this case, one has: $|A(e_2)| < |A(e_1) + A(e_3)|/2$, as in figure 2 and the median hydrophobic layer occupies an area smaller than the mean area of the two surrounding hydrophilic layers.

On the contrary, when M_1, M_2, M_3 lie within the segment CC', the parallel surfaces are locally hyperbolic (figure 1), the bilayer being *saddle-shaped*, and $|A(e_2)| > |A(e_1) + A(e_3)|/2$ (figure 2). Thus the median hydrophobic layer occupies an area larger than the mean area of the two surrounding hydrophilic layers. These inequalities also hold for three successive and equidistant levels e_1, e_2, e_3 defined in a monolayer. A layer sandwiched between two other layers is larger than the average of these two layers, if saddle-shaped (to take this example), whatever the hydrophilic or hydrophobic nature of this layer.

These inequalities may not be very important in smectics formed by very tight stacks of bilayers, whose radii of curvature are large with respect to the layer thickness. On the contrary, these inequalities are essential for strongly deformed bilayers forming very small vesicles or highly toroidal surfaces.

5. Polarized and non-polarized spontaneous curvatures

The spontaneous curvature usually considered in bilayers is a splay c_0 originating from the area difference separating the two monolayers, and observed in most biological cell membranes, with phospholipids distributed at different concentrations in the two monolayers. This asymmetry is generally reinforced by proteins and polysaccharides associated to biological membranes. This means that the splay energy is minimised when $c + c' = c_0$. Helfrich and Deuling were able to account for the biconcave shape of red cells or discocytes by assuming the membrane to have a spontaneous splay c_0 of such a sign that it everywhere represents an outward concavity [9]. This spontaneous splay is generally absent when bilayers are prepared *in vitro* from purified amphiphilic compounds or their mixtures, since there are no reasons to get such differentiations between the two monolayers.

The above considered inequalities indicate that another origin is possible for a spontaneous hat shape in bilayers. Consider a bilayer made of two identical monolayers, with a molecular structure and surrounding chemical conditions leading to a paraffinic layer whose area is less than the mean area of the two associated hydrophilic levels. In that case, a small disc of this bilayer adopts a hat shape, whose concavity is chosen either in one or in the opposite direction. This is a *non-polarized spontaneous hat shape* which occurs when the molecules in excess in one of the two monolayers of the disc can be 'accepted' by the rest of the bilayer, by lateral diffusion or by an eventual but rare flip-flop [10]. In general, the local shape of a bilayer results from spontaneous factors which show a polarity as c_0, but also from an excess or a deficit of area of the hydrophobic layer compared with the mean area of the hydrophilic levels.

It is worth remembering that biconcave vesicles were observed in bilayers with $c_0 = 0$ [11]. The discocyte shape associates elliptical hats at the periphery, plus two opposite spherical shapes about the axis and two circular narrow bands of saddle-shaped membranes. The preponderance of hat-shapes can be due to an area deficit of the hydrophobic median layer. The area excess of the outer monolayer along the curved peripheral cylinder can be partially compensated by an area loss along the two spherical areas. The biconcave vesicles with $c_0 = 0$ are a strong argument for assuming not only a spontaneous mean curvature, $1/2(1/\rho + 1/\rho')$, which is a splay, but also a spontaneous *gaussian* curvature, $1/\rho \ 1/\rho'$ which is a saddle–splay, to be an intrinsic property of the membrane.

6. Mean curvature and gaussian curvature

Consider now three parallel and equidistant surfaces at levels e, 0 and $-e$, as in bilayers. From equation (1), one finds:

$$[A(e) - A(-e)]/2e = c + c' \qquad (2)$$

and

$$[A(e) + A(-e) - 2A(0)]/2e^2 = cc'. \qquad (3)$$

For e very small, this gives:

$$c + c' = \mathrm{d}A(0)/\mathrm{d}e \tag{4}$$

and

$$2cc' = \mathrm{d}^2A/\mathrm{d}e^2. \tag{5}$$

The term $c + c' = 1/R + 1/R'$ is the *splay* of the unit vector **n** normal to the layer along Σ_0, and is twice the *mean curvature* $(c + c')/2$. The term cc' is the gaussian curvature and we can write these two relations as follows:

$$c + c' = [\mathrm{d}S(e) - \mathrm{d}S(-e)]/2e\mathrm{d}S(0) \tag{6}$$

$$cc' = [\mathrm{d}S(e) + \mathrm{d}S(-e) - 2\mathrm{d}S(0)]/2e^2\mathrm{d}S(0). \tag{7}$$

Integrating the second equation over a closed surface Σ_0, of area $S(0)$, p being the number of separate parts and t that of toroidal handles, the Gauss–Bonnet theorem gives:

$$\int_{\Sigma(0)} cc'\mathrm{d}S_0 = 4\pi(p - t) = [S(e) + S(-e) - 2S(0)]/2e^2 \tag{8a}$$

or

$$S(e) + S(-e) - 2S(0) = 8\pi e^2(p - t) \tag{8b}$$

$S(e)$ and $S(-e)$ being the areas of surfaces $\Sigma(e)$ and $\Sigma(-e)$ parallel to $\Sigma(0)$ at a distance e sufficiently short to avoid singularities. For a simply closed surface, with a topology which is that of the sphere, $p = 1$ and $t = 0$, and one has: $S(e) + S(-e) = 2S(0) + 8\pi e^2$, the deficit of $S(0)$ with respect to $[S(e) + S(-e)]/2$ being $4\pi e^2$, which is not negligible for strong curvatures, in very small vesicles for instance. For closed surfaces topologically equivalent to a simple torus, $S(e) + S(-e) = 2S(0)$.

The volume occupied by an amphiphilic molecule within a mono- or a bi-layer is constant at a given temperature. A narrow prism of bilayer, with its lateral faces normal to the bilayer has a volume calculated from the formula of the three levels:

$$\mathrm{d}V_b = [\mathrm{d}S(e) + \mathrm{d}S(-e) + 4\mathrm{d}S(0)]e/3. \tag{9}$$

This gives for a monolayer with the levels e, $e/2$ and 0:

$$\mathrm{d}V_m = [\mathrm{d}S(e) + \mathrm{d}S(0) + 4\mathrm{d}S(e/2)]e/6 \tag{10}$$

and it is worth remembering that $\mathrm{d}S(0) = 0$ in spherical or cylindrical micelles.

From equations (6), (7) and (9), one finds useful equations for bilayers or membranes, associating the external hydrophilic area, the lipophilic area, the volume and the gaussian curvature:

$$[\mathrm{d}S(e) + \mathrm{d}S(-e)]/2\mathrm{d}S(0) = 1 + e^2cc' \tag{11}$$

$$[\mathrm{d}S(e) + \mathrm{d}S(-e)]/\mathrm{d}V_b = 3(1 + e^2cc')/e(3 + e^2cc') \tag{12}$$

and

$$\mathrm{d}V_b/\mathrm{d}S(0) = 2e(1 + e^2cc'/3). \tag{13}$$

These purely geometrical relations, derived from properties of parallel surfaces, indicate that the gaussian curvature cc' strongly depends on the physicochemical conditions, which for a given number of amphiphilic molecules and at constant temperature control the corresponding volume $\mathrm{d}V_b$, the external hydrophilic area $\mathrm{d}S(e) + \mathrm{d}S(-e)$, and the median area $\mathrm{d}S(0)$.

7. The two spontaneous principal curvatures

In the rest of the paper, we call e the half thickness of a bilayer and to come back to figure 2, we choose $e_2 = 0$ for the median level of a bilayer, and $e_3 = +e$ and $e_1 = -e$ for the two external levels. As indicated above, to avoid singularities within a bilayer, $A(-e)$, $A(0)$ and $A(e)$ have to have the same sign, cf. figure 1. $S(0)$ being chosen positive, $S(e)$ and $S(-e)$ are also positive, and therefore also $A(0)$, $A(e)$ and $A(-e)$, whatever the bilayer shape, hat or saddle.

$S(e)$ and $S(-e)$ are defined within a given physicochemical environment, for a small disc of bilayer *in its relaxed state*, of median area $S(0)$ and thickness $2e$.

From the above relations (2 and 3), we see that c and c' are the roots of the equation

$$2e^2c^2 - ec[A(e) - A(-e)] + [A(e) + A(-e) - 2A(0)] = 0 \tag{14}$$

and these roots are real, if the discriminant is positive or zero:

$$[A(e) - A(-e)]^2 \geqslant 8[A(e) + A(-e) - 2A(0)]. \tag{15}$$

The situation is represented in an x, y diagram (figure 3), with $x = A(e)$ and $y = A(-e)$, and $A(0) = 1$. The inequality (15) can be written differently:

$$A(e) + A(-e) \leqslant 2A(0) + [A(e) - A(-e)]^2/8 \tag{16a}$$

or

$$x + y \leqslant 2 + (x - y)^2/8 \tag{16b}$$

and the existence of real roots is verified for points lying outside or along the parabola, whose symmetry axis is the line $y = x$, and which is tangent to the x axis at point $x = 4$, and symmetrically to the y axis, at point $y = 4$.

The inequality (15) is always satisfied by a small disc of a naturally saddle-shaped bilayer, since $A(e) + A(-e) - 2A(0)$ is then negative and the equation (7) has two real roots $\gamma = 1/\rho$ and $\gamma' = 1/\rho'$ of opposite signs, which are *two spontaneous principal curvatures or principal splays*.

When $A(e) + A(-e) - 2A(0)$ is positive, the bilayer is hat-shaped. The discriminant is positive above the line

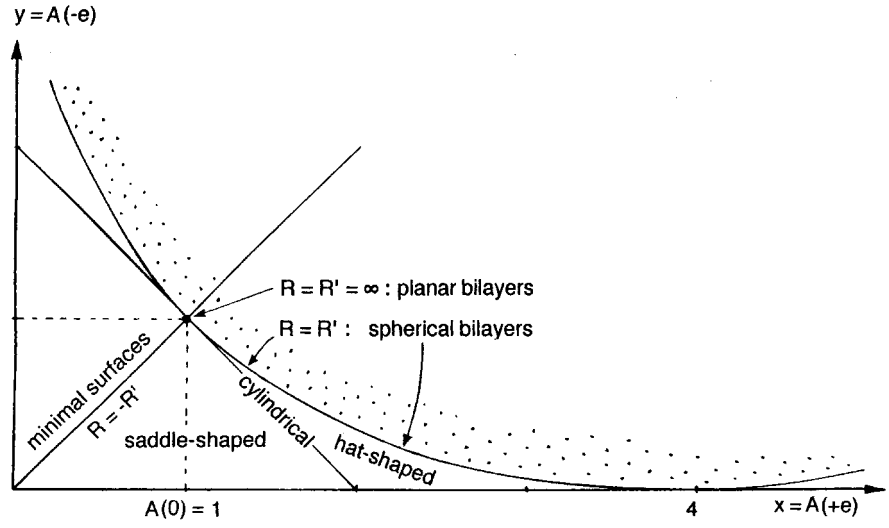

Figure 3. Bilayer local shape as a function of $A(e)$ and $A(-e)$ for $S(0)$ constant. The dotted region corresponds to impossible deformations, with imaginary curvature radii.

$x + y = 2$, and below the parabola, whereas it is zero along it. Again, this allows one to define in this domain two spontaneous principal curvatures or splays of like signs, γ and γ', for a small bilayer disc adopting a hat shape in its relaxed state. The diagram is obviously limited to $A(e)$ and $A(-e)$ positive, and we can choose $A(e) > A(-e)$, without loss of generality, which reduces the diagram to a 45° sector. Since we also suppose that the caustics do not penetrate the bilayer, it follows that, in the hat domain, the curvature radii R and R' are larger than e and we can write $R > R' > e > 0$, also without loss of generality. From equations (2 and 3), we deduce:

$$[A(e) + A(-e) - 2A(0)]2e^2 = (RR')^{-1} < e^{-2} \tag{17a}$$

or

$$A(e) + A(e) - 2A(0) < 2 \tag{17b}$$

and *a fortiori* $A(e) < 4A(0)$, which limits the study to $A(e) \leqslant 4$, at the contact point of the parabola with the x axis. In figure 3, the hat and saddle domains are separated by the straight line $x + y = 2$ corresponding to the locally cylindrical shapes. Spherical shapes lie along the parabola segment, the locus of double roots, where $c = c'$. The x axis corresponds to $R' = e$ and the curvature centre C' lies within one of the two hydrophilic levels, which corresponds to a local infinite curvature. Therefore, the x axis and its close vicinity must be excluded from the hat and saddle domains, as leading to prohibitive energies. On the contrary, the arc of parabola limiting the imaginary domain is however realistic, since it corresponds to planar bilayers at the top of the domain, transforming into spherical shapes along the parabola arc, but its extremity with a tangential contact at a point of the x axis must be excluded, like the rest of the x axis, due to an infinite curvature. The straight segment along $y = x$, within the 'saddle domain' corresponds to minimal surfaces with $R = -R'$.

8. Origin of shape similarities at different scales

To summarize, a freely deformable disc of a bilayer shows two spontaneous curvatures γ and γ', whose sum and product are:

$$\gamma + \gamma' = c_0 = [A(e) - A(-e)]/2e \tag{18}$$

$$\gamma\gamma' = g_0 = [A(e) + A(-e) - 2A(0)]/2e^2. \tag{19}$$

They depend on $A(e)$ and $A(-e)$, i.e. on $\mathrm{d}S(e)$ and $\mathrm{d}S(-e)$ imposed by the physicochemical environment for a given $\mathrm{d}S(0)$, in the absence of any other external constraint on the bilayer disc. The two spontaneous curvatures γ and γ' are the roots of $c^2 - c_0 c + g_0 = 0$ which are real when $g_0 \leqslant c_0^2/4$. Despite this simple presentation, we prefer the $A(e)$, $A(-e)$ diagram, rather than the c_0, g_0 one, since $A(e)$ and $A(-e)$ depend directly on the physicochemical environment.

The usual theories simply compare $\mathrm{d}S(e)$ and $\mathrm{d}S(-e)$ [12] in order to show how a disc of hat-shaped bilayer transforms into a planar one and then into a cup, which means a hat of opposite concavity, the hats being restricted to the lower 45° sector of figure 3 and the cups to the upper 45° sector. The three levels theory presented here distinguishes between hats, saddles, cylinders and all local shapes encountered. The diagram $x = A(e)$, $y = A(-e)$ also presents a symmetrical distribution with respect to the line $y = x$, as in the two levels theories.

Similarly, the comparison of areas at three levels e_1, e_2, e_3, lying parallel and equidistant within the structure of *an amphiphilic monolayer*, leads to the construction of an analogous diagram and to the definition of two radii of spontaneous curvature. Biological

membranes and monolayers are both dissymmetrical and differ from *in vitro* assembled bilayers, which are symmetrical. The two spontaneous splays γ and γ' are equal and opposite in these 'synthetic' bilayers, whereas they differ in absolute value in monolayers and in biological membranes. This means that the geometrical ingredients of shape are identical in micelles and in biological membranes, with only a change of scale. However, it occurs that symmetrical bilayers form analogous shapes, even in the absence of a spontaneous splay c_0, the spontaneous gaussian term g_0 creating either hats or saddles according to its sign, positive or negative.

9. Plausible shapes of micelles and vesicles

The only known surfaces showing two constant principal curvatures are spheres, cylinders and planes. These shapes are those mainly observed in lyotropic systems: spherical micelles or vesicles, cylindrical micelles or bilayer tubes, planar monolayers or bilayers, where $c + c'$ and cc' are constant, but generally different from $\gamma + \gamma'$ and $\gamma\gamma'$, the elastic constraint being uniformly distributed within these micelles and bilayers. A spherical micelle, a cylindrical one and a bilayer are represented in figure 4(*a*, *b*, *c*); with their radii deduced from the V/AR ratio (V and A being constant), the cylinder radius is equal to the bilayer thickness, whereas the sphere diameter is triple the bilayer thickness. As stated above, however, these differences between R_S, R_C and R_B are probably attenuated. These very different aggregates are obtained with the same amphiphilic compound, when the length of the hydrophobic part can vary, due to chain melting for instance, or if interdigitation is possible as in figure 4(*c*), or both; or also when other arrangements are made possible with cosurfactants, for example.

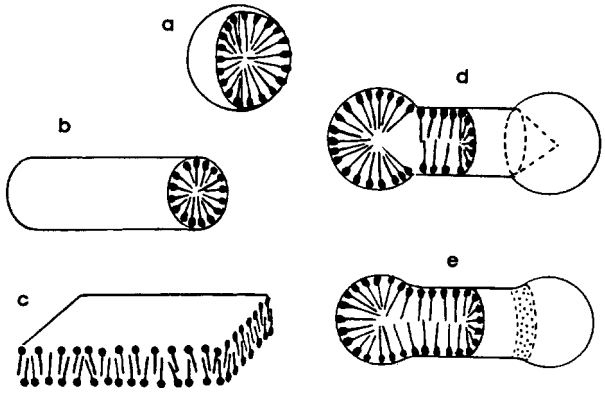

Figure 4. Main morphologies of lyotropic aggregates. (*a*) Spherical micelle, (*b*) cylindrical micelle, (*c*) bilayer, (*d*) elongated micelle associating spherical extremities to a cylindrical segment, with empty cavities, (*e*) rehandling of the elongated micelle, with a radius decrease at the spherical ends and a continuous tilt of molecules along a toroidal belt (dotted zone).

The other observed aggregates are elongated micelles, branched micelles, ribbons, discs, etc. and these associate several parts which are spherical, cylindrical, planar or toroidal. For instance, an elongated micelle can be considered as made of a cylindrical segment and two hemispheres; similarly, a ribbon is a bilayer with two hemicylindrical edges, and a disc is a circular piece of bilayer limited by a half cylinder, circularly bent [13]. Actually, these schematic models need to be modified, since they suppose that $R_S = R_C = R_B$, whereas we have indicated in the introduction that we have $R_S > R_C > R_B$, with important differences. This leads one to consider shapes built with sphere and cylinder pieces, whose dimensions are as in figure 4(*a*, *b*), but this creates an empty space in the 'dumb-bell' micelle represented in meridian section in figure 4(*d*). To avoid this situation, toroidal zones are introduced to bind the different parts of micelles, without discontinuities of the molecular orientations, in order to attenuate the difference between R_C and R_B, this requiring the possibility of slight molecular tilts in this region, figure 4(*e*). Spherical and dumb-bell shapes are also found in vesicles made of a single bilayer (figure 5) or of several nested bilayers. We observed them in lecithin–water preparations, but many micrographs were published before in the literature, from Nageotte in 1937 [14] to recent work, in particular those due to Sekimura and Hotani [15].

10. Size and shape parameters of micelles and vesicles

These micellar shapes are defined geometrically by a series of parameters which are radii of curvature or other lengths. According to the micellar type, one, two, three or more parameters may be necessary and this is illustrated in figure 6. A unique parameter, the radius R_S, completely determines the dimension of a spherical micelle, figure 6(*a*); for a cylindrical micelle, this will be the radius R_C, figure 6(*b*). Two parameters are required to specify the shape and size of an elongated micelle, forming statistically an ellipsoid of revolution with two radii R_L and R_R, the longitudinal one and the transverse one, figure 6(*c*). Three parameters are involved in the shape and size of a dumb-bell micelle, if the structure is simplified to a cylinder of length L and radius R_C, linking two spherical extremities of radius R_S, figure 6(*d*). A supplementary radius R_T is introduced, figure 6(*e*), when a toroidal belt joins the cylinder to its spherical extremities, as in figure 4(*e*). A junction of three cylindrical micelles, generally separated by 120° angles, is defined mainly by two radii, that R_C of the cylinders and that R_T as shown in figure 6(*f*). Since for a micelle (monolayer) such a junction can be the nucleation centre of a bilayer structure, a slight depression D is often

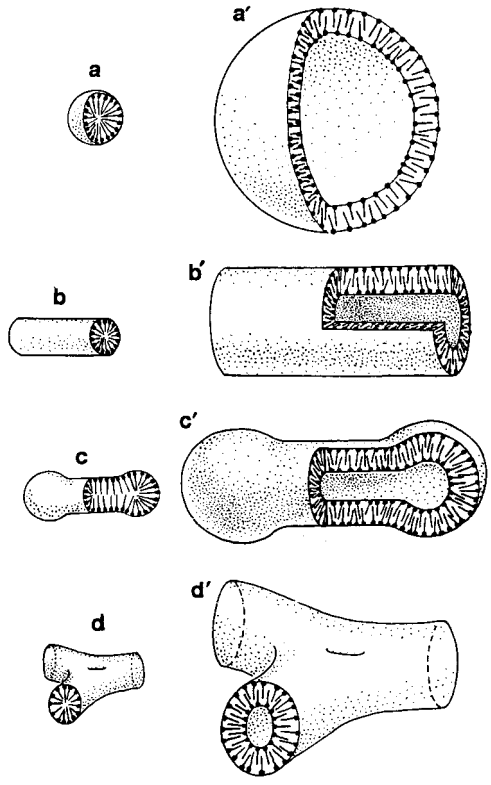

Figure 5. Comparative morphology of micelles and bilayer systems: micellar shapes are often reproduced by bilayers, at a larger scale. (*a*) Spherical micelle (with a paraffinic core), (*a'*) spherical vesicle made of a bilayer enclosing water, (*b*) cylindrical micelle (with a paraffinic core), (*b'*) cylindrical tube of bilayer (enclosing water), (*c*) a micellar dumb-bell (paraffinic core), (*c'*) a vesicular dumb-bell (water core), (*d*) branching cylindrical micelle, (*d'*) branching of a bilayer tube.

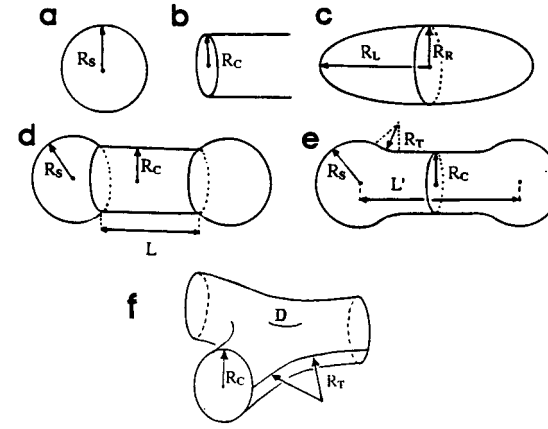

Figure 6. Main morphological parameters in the description of micelles, vesicles and liposomes. These parameters are mainly radii or lengths: the sphere radius R_S in (*a*), the cylinder radius R_C in (*b*), the longitudinal radius R_L of the ellipsoid and the radius R_R of the circular section normal to R_L in (*c*). In (*d*), similar radii are used for the dumb-bell description, R_S and R_C, plus the cylinder length L. These three parameters do not suffice, if we take into account the presence of toroidal annuli as in figure 4(*e*). It is then more convenient to use the length L' separating the two centres of the spherical ends. Similarly (*f*), two parameters R_C and R_T allow one to describe a branching node and are, respectively, the cylinder radius, and the tore radius along a generator in the plane of the three cylinder axes; a third parameter is necessary if one takes into account the depression D due to the nucleation of a bilayer structure in the core of the bifurcation.

present in the core and the thickness along the axis is also a useful parameter in the description.

The representations of figure 7 correspond to the main shapes obtained from a monolayer (*a*) producing the three *basic shapes*, the sphere (*b*), the cylinder, rigid (*c*) or flexible (*d*), and the plane (*e*). Their association leads to a *zoology* with *two classification principles*; *the global shape*, which is *isometric*, *flat* or *elongated* and the *complexity* defined here by the number of parameters. Arrows indicate a set of plausible transformations and one gets a kind of *evolutionary tree*. Like most classifications, it does not work perfectly and the form (*x*) for instance can be derived from the sphere, as well as from the cylinder. The number of parameters depends on the description accuracy, as indicated above for the dumb-bell shape (*o*) and the triple junction (*i*). This also holds for the other shapes requiring more parameters in their definition.

Most shapes, figure 7 (*o–h, l, m, o–x*) are obtained from a sphere, by continuous deformation, with elongation, flattening or branching and are topologically equivalent. For the various types of junctions (*i–k, y*), monolayer recombinations are necessary and also for (*z*), with bilayer recombinations. This often produces systems of highly toroidal bilayers showing in general a constant mean curvature, but variable gaussian curvature. Among the examples, there are the periodical minimal surfaces found in many cubic phases of water–lipid systems and also sponges, about which the question remains as to whether the median bilayer surface is exactly minimal.

Most of these shapes are observed in simple or multilayered vesicles or liposomes. Tetrahedral micelles or liposomes such as that of figure 7(*x*) are not very likely to exist, since they associate spherical and strongly saddle-shaped interfaces. This situation is realized at a lower degree in figure 7(*u, v*) and was observed in liposomes by Sekimura and Hotani [15]. The cup shape of figure 7(*r*) is known in red cells or in vesicles called 'stomatocytes', but this shape applied to a micelle corresponds to an open vesicle, which is generally considered as an unstable situation, and the system is 'supposed' to reclose rapidly, but this probably depends on the elastic rigidities and spontaneous curvatures. In biological systems, highly toroidal bilayers also form cubic phases, but the bilayer median surface is not minimal, due to

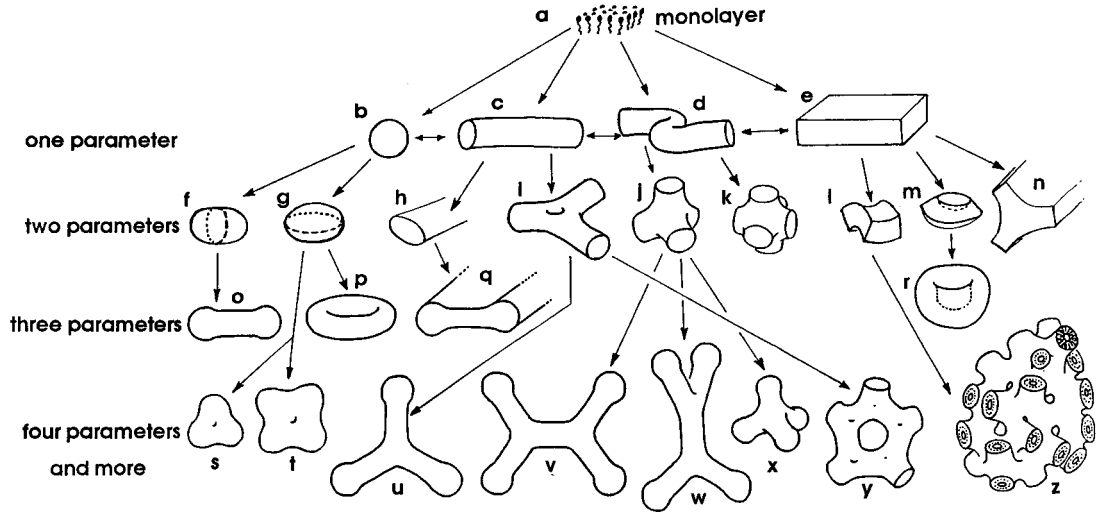

Figure 7. The lyotropic 'microzoology' or the main shapes *observed* or *supposed to exist* in micelles, and generally observed on a larger scale in vesicles and liposomes. They are ordered according to their complexity (minimal number of parameters to define the shape and size) and according to a morphological trend, the structure being derived either from the sphere, the cylinder or the plane. a: The monolayer or 'primordial' pattern. b: Sphere. c: Rigid cylinder, with a circular cross section. d: Flexible cylinder. e: Planar layer. f: Elongated revolution ellipsoid (rugby ball). g: Flattened revolution ellipsoid. h: Cylinder with an elliptical cross section. i: Triple junction, with a slight depression in the core. j: Quadruple junction (tetrahedral). k: Sextuple junction (octahedral). l: Saddle-shaped layer. m: Hat-shaped layer. n: Triple layer junction. o: Dumb-bell. p: Discocyte (biconcave). q: Ribbon with cylindrical edges. r: Stomatocyte. s: Rounded triangle. t: Rounded square. u–x: Branched dumb-bells, with coplanar branching or in two perpendicular planes. y: Reticulum. z: Sponge structure obtained with spontaneously saddle-shaped bilayers.

composition differences between the two monolayers; the membrane rather conforms to a constant mean curvature surface, indicating a likely constant pressure difference between the two separated water compartments (references in [8(*a*)]).

11. An example of membrane polymorphism in living cells

As indicated above, bilayers present in biological systems arrange into shapes similar to those found in micelles, but on a larger scale, each length being multiplied by a factor of about 10, with large variations. The best example of membrane polymorphism that we know is illustrated in figures 8 and 9, showing a particular type of secreting cells, studied in transmission electron microscopy in thin sections of resin-embedded material. This was observed in cells of the shore crab epidermis, within secretion granules developing in the early phases of the moulting cycle. Similar cells were described in the crayfish epidermis, in a sense organ, the statocyst [16], and also in epidermal glands near the eyestalk of lobsters or close to the abdomen pleopods [17(*a*)]. Similar granules are sometimes found in crustacean haemocytes [17(*b*)]. The secretion granules presented here contain sets of membranes forming swollen systems of parallel layers, planar or nested concentrically, or bilayer tubes of variable diameter arranging into regular hexagonal arrays or at random (figure 8). In other granules, tubes follow sinuous contours, branching or not, often associating into complex networks, figure 9(*a*, *b*, *c*).

Cell membranes are known to be made of phospholipidic bilayers to which are associated high contents of proteins and polysaccharides, with an asymmetric distribution. A good resolution on the scale of the bilayer itself, which is 50 Å thick, was made difficult by the presence of these macromolecules. Each granule differs from the other, either by the type of order, or by parameters such as tube diameter. This seems to be possible, since each granule is isolated by a closed bilayer from the cytoplasm and from the other granules.

12. Plausible reticulation of elongated micelles

Among the remarkable patterns revealed by these secretory cells, two must be considered more precisely: (1) bilayer tubes joining into 2D periodic networks, which superpose as do bilayers in swollen smectics; (2) branching bilayer tubes forming 3D networks, which are also known in many other biological structures [18].

This suggests the existence of similar geometries in networks of branched cylindrical micelles, and particularly: (1) systems of superposed layers made of reticulated cylindrical micelles; (2) cylindrical micelles forming 3D networks.

The 3D-networks of bilayer tubes or of cylindrical micelles exist in lyotropic cubic phases or in sponges, and one can easily verify that they represent inverse

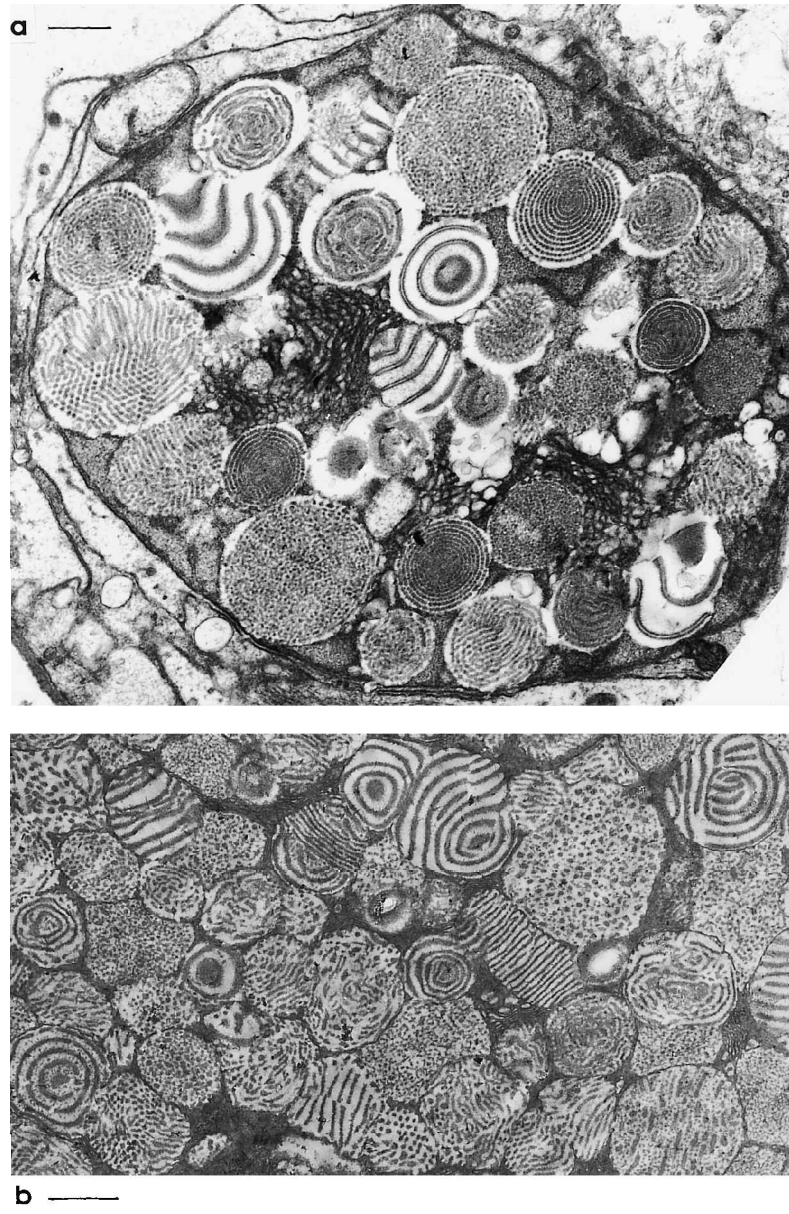

Figure 8. Secretory cell in the epidermis of *Carcinus maenas*, the shore crab. Epidermis of the branchial cavity was fixed with 4% glutaraldehyde in cacodylate buffer at pH 7.3, for 1 h and post-fixed with 2% OsO_4 in barbital buffer, at the same pH and for 15 min. Bars = 1 μm. (*a*) A cell filled with secretion granules made of membranes arranged according to ordered (hexagonal, lamellar…) or random patterns. (*b*) Another view showing many defects (edge or screw dislocations in the lamellar patterns).

phases. Both are supposed to exist in systems consisting of water and the amphiphilic drug amiodarone and in other lyotropic compounds of pharmaceutical interest [19–21].

13. Four types of swelling in lyotropic networks

A bilayer forming a periodic minimal surface (PMS), generally cubic, separates two water compartments, which can be considered as a set of tubes associating by their extremities at triple, quadruple or sextuple junctions, according to the PMS type, and the axial segments of these tubes join similarly to form a labyrinth lying in water [22]. Actually, there are two intertwined labyrinths corresponding to the two water compartments and the situation is topologically similar for sponges. Such systems are said to be bicontinuous, the bilayer being continuous and multiconnected, separating two water compartments which are themselves continuous and multiconnected. In the inverse phases, one has oily labyrinths instead of water labyrinths, and the amphiphilic molecules form two intertwined networks of cylindrical micelles, separated by a toroidal surface lying in water.

There are four possible types of swelling for such phases, differing by the nature of the swelling agent (water or oil) and by the localization of swelling along the toroidal surface, or along the axes of labyrinths. There is also the possibility of a double swelling by water and by oil. When swelling is important along the toroidal surface, with cylindrical micelles (direct or inverse)

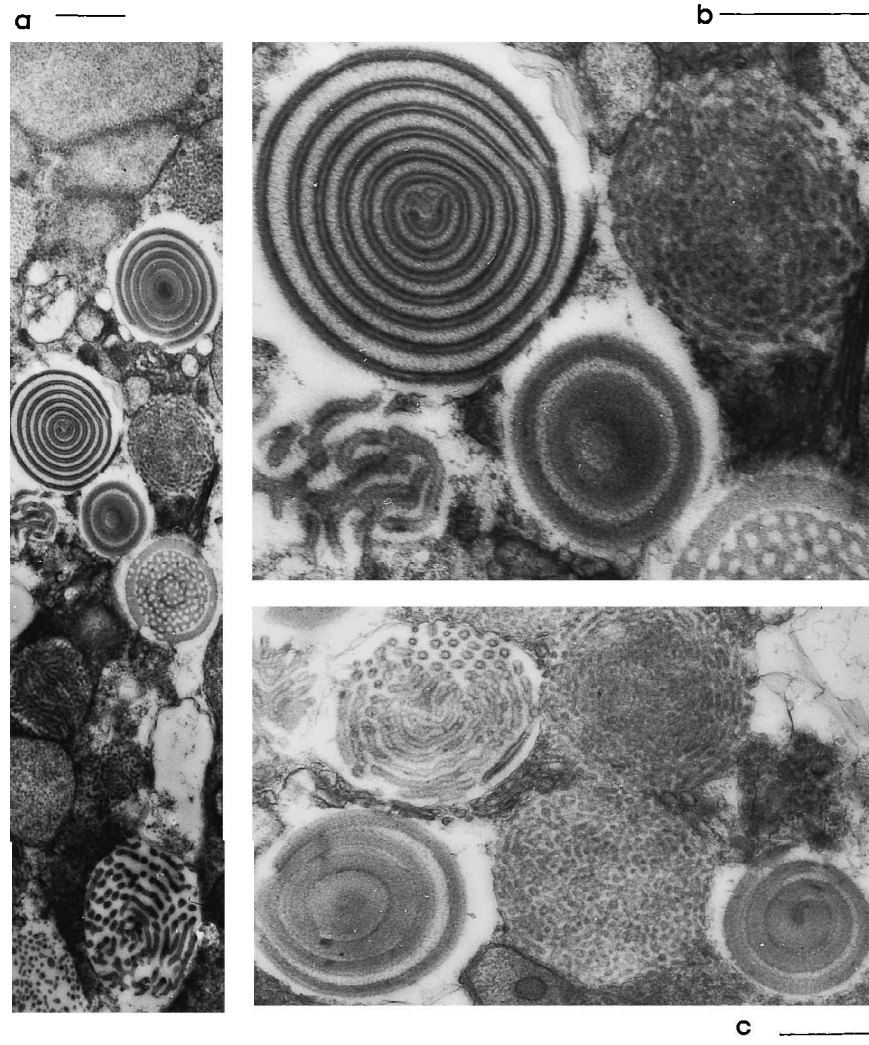

Figure 9. *Carcinus maenas*, as in figure 5. a: Some secretory granules in different section planes, passing through the centre, or almost tangentially. b: At higher magnification, the materials associated to membranes resemble a glycocalyx of cell membrane, known to be made of polysaccharides. The granule at top left shows an edge-dislocation. Just below is a set of branched tubes of bilayers and, at the bottom right, there are pairs of membranes forming a reticulum. c: At top left, a round granule with flexible tubes more or less aligned and seen in longitudinal view or in cross section.

arranged into a loose 3D lattice, the two labyrinths probably cease to form separate entities, since breaks and recombinations occur without distinction between the two networks.

14. The Winsor model and its geometrical consequences

Lamellar phases were often observed to occur between two viscous cubic phases and this was discussed by Winsor [1] and Scriven [23] in their presentation of the lyotropic polymorphism and phase transitions encountered along the concentration axis of a unique and 'ideal' amphiphilic component.

At low concentrations, but higher than the critical micellar concentration (CMC), amphiphilic molecules assemble into spherical micelles, separated by water, and they arrange themselves into centred cubic networks, when repulsion forces are sufficient (figure 10, S_{1C}). A concentration increase generally results in elongated and cylindrical micelles, which align and form hexagonal arrays (figure 10, M_1). At higher concentrations, branching of cylinders occurs, with cylindrical segments joining three by three, four by four (figure 10, V_1) or six by six, to give another type of centred cubic lattice [24]. The lamellar phase then differentiates (figure 10, G) and a further increase of lipids leads to the sequence of the inverse phases, successively the cubic arrangements of segments V_2, but now with water along the cylinder axes, and finally the inverse hexagonal phase M_2 and the inverse micelles S_{2C}.

In real diagrams, this phase series is not complete, some phases being absent or replaced by others, a columnar phase (rectangular or tetragonal) for instance, instead of a hexagonal one.

It must be pointed out that new lyotropic phases have been discovered [25], some of them showing a similar topology, whereas the discrete order of micelles is lost. A centred cubic array of spherical micelles can be replaced by a random arrangement of these micelles (figure 10, S_1). Similarly, the hexagonal or rectangular

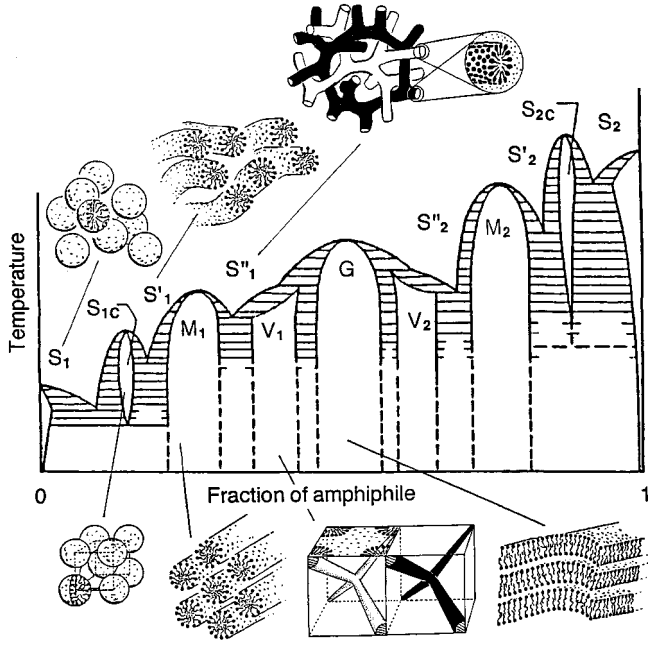

Figure 10. Idealized phase diagram of a water-lipid system, redrawn from [1], [2] and [18] and completed by representations of classical phases encountered, when the surfactant concentration is increased progressively from 0 to 100%. S_1C: Cubic micellar phase. M_1: Hexagonal phase. V_1: Bicontinuous cubic phase. G: Lamellar phase. V_2: Inverse bicontinuous cubic phase. M_2: Inverse hexagonal phase. S_2C: Inverse micellar cubic phase. A temperature increase leads to isotropic sols or gels S_1 corresponding for instance to globular micelles randomly dispersed in water. S_1' could correspond to a disordered set of cylindrical micelles and S_1'' to a network of branching micelles the topological equivalent of a bicontinuous cubic phase. The phases S_2 correspond to the inverse structures.

order of elongated micelles can be lost and the symmetry is then nematic (figure 10, S_1'), or isotropic if the orientational order itself is lost. Sponges have the topology of bicontinuous cubic phases, but differ from them by the absence of cubic order (figure 10, S_1''), etc.

In his idealized phase diagram, Winsor included the amorphous solution phases encountered at higher temperatures and also the eutectics alternating with frozen phases at lower temperatures [1]. In between lie the lyotropic mesophases, supposed to present a discrete order whereas, at the level just above, the discrete order is lost, but possibly not the topology, as represented in figure 10 (for the various S, S′ and S″, with indices 1 or 2).

R is a parameter indicating the tendency of an amphiphilic monolayer to become convex, either towards its polar environment ($R<1$), or towards its lipophilic environment ($R>1$) [1]. This divergence in one direction, or in the opposite, is expressed geometrically by the local mean curvature C, a monotonous function of R, which can be chosen positive for diverging polar heads and negative for diverging lipophilic tails. R is always positive and $R<1$ corresponds to $C>0$, whereas, for $R>1$, one has $C<0$. The consequence is that, in a first approximation, the mean curvature C of a monolayer is also a monotonous function of the concentration of the amphiphilic compound in water, with some exceptions, and an example will be considered below.

Let us return to figure 4 and consider for the different micelles an outer smooth surface corresponding to the average position of the van der Waals contours of the polar heads. This surface is a sphere of radius R_S in a spherical micelle, figure 6(*a*), a cylinder of radius R_C in a cylindrical micelle, figure 6(*b*), etc. In spherical micelles, the mean curvature is $1/R_S$. The passage to elongated micelles, and finally to cylindrical ones, leads to the differentiation of two local principal curvatures, with a zero curvature in the longitudinal direction and a transversal curvature $1/R_C$. The decrease of the mean curvature C from its value C_S, in a spherical micelle, to the value C_C, in a cylindrical one, leads one to write: $C_S = 1/R_S > C_C = 1/2R_C$, from which one deduces that $R_C < R_S < 2R_C$. Branching introduces saddle-shaped surfaces with two principal curvatures of opposite signs, which are approximately $1/R_C > 0$ and $1/R_T < 0$, as shown in figure 6(*f*), with $|R_T| > |R_C|$, the mean curvature being positive. If the branching results in a reticulating process, the monolayer becomes toroidal and this increases the ratio of saddle-shaped surfaces in the micellar system, figure 7(*y*). The mean curvature C_R of branched and reticulated micelles associates two opposite principal curvatures, but is still positive. The central part of the branching is the nucleation centre of a bilayer, which can develop with a mean curvature C_B close to zero. The successive mean curvatures C_S, C_C, C_R, C_B form therefore a decreasing series:

$$C_S = 1/R_S > C_C = 1/2R_C > C_R$$
$$= (1.2R_C) - (1/2R_T) > C_B \sim 0.$$

Note that two hollows D can appear symmetrically, figure 6(*f*), along the threefold axis of a branching with two hat shapes, presenting a local negative curvature, and in the case of monolayer micelles these branching nodes can be nucleation centres of bilayers. This indicates a possible exception to the monotone evolution of the mean curvature.

For the following inverse phases, another series of inequalities can be written, the mean curvatures C_{S-}, C_{C-}, C_{R-} and radii R_{S-}, R_{C-} being now considered as negative and R_{T-} positive:

$$C_S = 1/R_{S-} < C_C = 1/2R_{C-} < C_R$$
$$= (1/2R_{T-}) - (1/2R_{C-}) < C_B \sim 0.$$

The mechanisms proposed by Winsor [1] also apply to the shape variations in *bilayers*. A tendency of the hydrophobic chains to converge within a bilayer, instead of lying parallel, means that the area of the median level is less than the mean area of the two external levels and the bilayer is locally *hat-shaped*, if it can adopt its spontaneous shape without external constraint. On the contrary, the bilayer is locally *saddle-shaped* , if there is a tendency of lipophilic extremities to diverge, with an area of the median layer larger than the mean area of the corresponding external layers. This suggests a series of transitions in the swelling of a smectic system of cell membranes, cf. the variations in dimension exemplified in figures 8 and 9 and also in the case of an amphiphilic drug such as amiodarone [20, 21]. As indicated above, in these conditions, bilayers and cell membranes can mimic on a larger scale the shape evolution encountered in micelles.

15. The curvature energy of bilayers

The elastic energy derived from the Oseen–Frank formula applied to an isolated bilayer or a membrane is usually written:

$$f = \mathrm{d}F/\mathrm{d}s = k(c + c' - c_0)^2/2 + k_g cc' \qquad (20)$$

with a spontaneous splay c_0, already considered, and two rigidities: the splay coefficient k, as in uniaxial liquid crystals, and another elastic constant k_g for the gaussian curvature cc' [5–7, 9–11]. The energy of a freely deformable bilayer disc shows a minimum when $\mathrm{d}f = k(c + c' - c_0)(\mathrm{d}c + \mathrm{d}c') + k_g(c\mathrm{d}c' + c'\mathrm{d}c) = 0$ and $\mathrm{d}^2 f > 0$, which leads to:

$$c = c' = c_0 k/(2k + k_g) \qquad (21)$$

with $\mathrm{d}f/\mathrm{d}c = c(2k + k_g) - kc_0$ and $\mathrm{d}^2 f/\mathrm{d}c^2 = 2k + k_g > 0$.

Helfrich considered the simple case of a spherical vesicle [6], with $c = c' = 1/r$ with an equilibrium for $c_{eq} = kc_0/(2k + k_g)$. In bilayers produced *in vitro*, $c_0 = c_{eq} = 0$, but stable spherical vesicles are often obtained, in a constrained state of energy $F = 4\pi(2k + k_g)$. Writing $\Delta c = c - c_{eq}$ and $\Delta c' = c' - c_{eq}$, Helfrich transforms equation (20) into:

$$f = k(\Delta c + \Delta c')^2/2 + k_g \Delta c \Delta c'. \qquad (22)$$

In our model, with two spontaneous principal curvatures, this can be considered as an invitation to replace in equation (20) the term $k_g cc'$ by something like $k_g(c - \gamma)(c' - \gamma')$ or $k_g(cc' - \gamma\gamma')$. There are two different ways to associate c and c' to γ and γ', and the idea is to choose the less energetic arrangement between $k_g(c - \gamma)(c' - \gamma')$ and $k_g(c - \gamma')(c' - \gamma)$. There is also the question of the k_g sign. The small piece of bilayer considered above, freely deformable with two spontaneous curvatures, submitted to curvatures c and c' so that the splay energy remains equal to zero ($\Delta c + \Delta c' = 0$), has a negative gaussian term since $\Delta c \Delta c' = -(\Delta c)^2$; but this corresponds to a deviation from the equilibrium value, and thus to a positive energy. The k_g modulus is therefore negative. Most measurements have given negative values for k_g [26, 27], but positive values were also considered for synthetic bilayers [28, 29] with $c_0 = 0$, and a spontaneous gaussian curvature implicitly supposed to be zero. In that case, a flat bilayer ($\gamma + \gamma' = \gamma\gamma' = 0$) has a zero energy after equation (22), but is unstable, since it transforms spontaneously into a saddle, k_g being positive. The only way to keep a positive energy for such deformations is to add a term $B(\partial u/\partial z)^2$ corresponding to a thickness variation of bilayers as in [28, 29]. It is true that deformations of layers can modify e, as suggested in equations (11–13).

More generally it is somewhat surprising to have an energy term $k_g cc'$ which easily changes its sign, the density f of the elastic energy being a function of c and c' represented by a paraboloid, which is elliptic if $2k + k_g > 0$ but hyperbolic if $2k + k_g < 0$, with level lines then drawing a saddle point corresponding to an unstable equilibrium. Our comparisons on the areas of the hydrophobic and hydrophilic levels lead one to consider the gaussian curvature term differently.

Bending mechanisms of biological membranes have been interpreted in terms of 'bilayer couples', the two monolayers responding differently to a perturbation [12], for instance by a variation of the area ratio of the two facing monolayers with the physicochemical environment. Actually, such models lead only to the production of hat-shaped surfaces. We prefer a three-layered model, with a median oily layer sandwiched between two hydrophilic ones, this being expressed by rewriting equations (6) and (7):

$$c + c' = \Delta_2 S_W/2eS_L \quad \text{and} \quad cc' = \Delta_3 S_W/2e^2 S_L. \qquad (23)$$

$S_L = S(0)$ represents the area of the lipophilic median level of a bilayer, $\Delta_2 S_W$ is the area difference (positive or negative) between the two outer layers in contact with water, inherited from the 'bilayer couple' model, $\Delta_3 S_W$ is an area difference involving the three layers: the excess or the deficit of the mean area of the outer layers with respect to that of the median layer.

The splay energy of a bilayer with local principal curvatures c and c', is

$$k(c - \gamma + c' - \gamma')^2/2 = k(c + c' - c_0)^2/2 = k[(\Delta_2 S_W/2eS_L) - c_0]^2/2.$$

The excess or deficit of mean area of the outer layers with respect to the inner one produces positive

energies, which are likely to be an even function of $(\Delta_3 S_W/2e^2 S_L) - \gamma\gamma'$, the square for instance; this leads to an energetic term such as $k_t(cc' - \gamma\gamma')^2$, with a coefficient $k_t > 0$ which is not independent from B, but is different from k_g whose physical meaning is not clear. This leads to a new expression for the elastic energy of bilayers and membranes, which can be adapted to monolayers or micelles:

$$dF/dS = f = k(c + c' - \gamma - \gamma')^2/2 + k_t(cc' - \gamma\gamma')^2. \quad (24)$$

The integration of this new biquadratic gaussian term $(cc' - \gamma\gamma')^2$ over a surface decomposes into three parts: that given by $k_t(\gamma\gamma')^2$ is proportional to the global bilayer area, that with $k_t\gamma\gamma'cc'$ is a Gauss–Bonnet integral, and that in $(cc')^2$ is the one of interest for comparisons between structures of identical topology and area, but of different shape. Note that equation (24) can be applied to monolayers, and associating them into a bilayer, this leads to a 'five layer theory' of bilayers and membranes, which can be compared with the three layer one. More terms then have to be introduced, but their discussion would be very long and we prefer to limit this consideration to a three-layered model. The need to consider a term such as $k_t(cc' - \gamma\gamma')^2$ emphasizes that we deal with very high curvatures, as in micelles, small vesicles, highly toroidal membranes, etc.

In principle, the lyotropic bilayers or monolayers considered here present a rotational symmetry C_∞, but the differences between the areas $S(+e)$, $S(0)$, $S(-e)$ lead to a *symmetry breaking* consisting in the differentiation of two principal curvatures.

Although several authors studied the origin of bilayers, starting from equation (20) or adding new gaussian terms as did Klösgen and Helfrich [30], such as $k_{II}(cc')^2$ and $k_{IV}(cc')^4$, they did not consider the possibility of two principal spontaneous curvatures, and therefore the introduction of a spontaneous gaussian curvature.

16. Shape determination

As indicated above, shapes with two constant principal curvatures are only spherical, cylindrical and planar, which could be one reason, among others, for their general presence in micelles and vesicles. Other shapes are encountered and particularly the toroidal junctions between these three basic shapes. The elastic energy presents a constant density f within monolayers or bilayers adopting such basic shapes. This density is f_S in a spherical end, f_C in a cylindrical segment or f_B in a planar structure; if c_S and c_C are the corresponding non-zero curvatures, equation (24) gives:

$$f_S = k(2c_S - c_0)^2/2 + k_t(c_S^2 - \gamma\gamma')^2$$
$$f_C = k(c_C - c_0)^2/2 + k_t(\gamma\gamma')^2$$
$$f_B = kc_0^2/2 + k_t(\gamma\gamma')^2.$$

These energies are minimized when $df_S/dc_S = df_C/dc_C = 0$, and this leads, for the cylinder, to $c_C = c_0 = \gamma + \gamma'$ and for the sphere to

$$k(2c_S - c_0) + 2k_t c_S(c_S^2 - \gamma\gamma') = 0 \quad (25)$$

which presents one real root at least. Knowledge of c_C leads to that of $\gamma + \gamma'$ and the value of c_S to that of $\gamma\gamma'$, if k_t/k is known.

The curvatures c_S and c_C can be obtained from direct observations of shapes in micelles and vesicles. This becomes possible and accurate by transmission electron microscopy of frozen hydrated specimens within a thin vitrified layer of water, by methods due to Chang *et al.* [31] and now applied to water–lipid systems [32].

Another approach to $\gamma\gamma'$ is possible from direct observation of micellar shapes, not only the radii of curvature, but also the length of cylindrical segments, as in figure 6(*d*, *e*). In a dumb-bell micelle, it can be seen that the ratio of the area occupied by the hydrophilic heads in contact with water over the volume of the amphiphilic material in the micelle is a simple function of L (a homographic one). The mean value of this ratio allows one to know that of cc', close to $\gamma\gamma'$; this is obtained from equations (12) or (13) written for bilayers, but easily adapted to monolayers. Knowing $\gamma + \gamma'$ and $\gamma\gamma'$, equation (25) then offers access to the ratio k_t/k.

17. Concluding remarks

Simple geometrical remarks on parallel equidistant surfaces show that a small disc of a bilayer, isolated in its physico-chemical environment, freely deformable without any other constraints than its elasticity, generally presents two spontaneous principal curvatures. This results in a local 'spontaneous shape' which is a hat, a cylinder or a saddle, and the principle also applies to monolayers, within micelles for instance. These spontaneous curvatures depend on the environment, temperature in particular and, in most cases, on ionic conditions.

The only surfaces presenting constant principal curvatures are the sphere, the cylinder and the plane. Micelles and lyotropic aggregates such as bilayers or biological membranes are often spherical, cylindrical or planar; they can also present more complex shapes by the association of differentiated parts which themselves are spherical, cylindrical or planar, and join along narrow zones—generally saddle-shaped.

The coexistence of different local shapes in a lyotropic aggregate requires the possibility of shape variations for

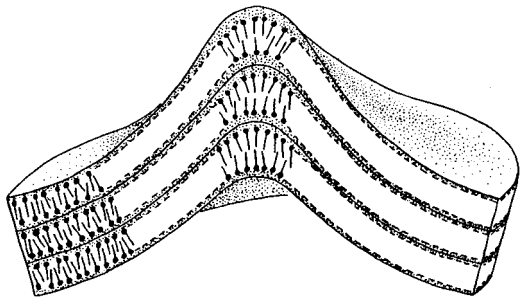

Figure 11. Set of three superposed bilayers in the presence of water (dotted areas), sectioned to display a focal region. Each unit, a bilayer plus the associated water, is limited by a solid line. Bilayers are toroidal and mainly saddle-shaped in focal domains, but hat-shapes are present and concentrated along the focal curves, corresponding here to the vertical axis. The bilayer thickness is strongly increased along this axis, with a lower degree of interdigitation of lipophilic ends and therefore a deficit of local mid-area S(0), which provokes the hat-shape. The intercalated water lamellae are thicker along this axis and are represented by the dotted areas.

molecules; this can be realized by molten paraffinic chains, or by segregation of molecules in a mixture such as lecithin which can modify the local 'spontaneous curvatures'. In the case of stiff hydrophobic chains, the passage from cylindrical micelles to bilayers generally requires an interdigitation of lipophilic ends. Spherical micelles often coexist with cylindrical ones, and these latter with planar bilayers, but the coexistence of the three shapes is less frequent. However, it remains possible to vary ionic conditions, cosurfactants, temperature, etc. and this can lead to remarkable lyotropic polymorphisms.

The consideration of hat shapes and saddle shapes is essential at the scale of micelles and small vesicles, but cannot be neglected at much larger scales. For instance, many amphiphilic compounds in the presence of water produce myelin figures easily observed between slide and cover slip. In these strongly hydrated textures, bilayers are mainly hat-shaped or cylindrical. After partial dehydration, by evaporation along the cover slip edge, oily streaks and polygonal fields appear, two textures where saddle shapes are preferred. The hat shapes are progressively limited to the close vicinity of focal curves and this requires a slight area decrease of the median oily layers, probably correlated with a loss of interdigitation and a thickness increase as represented in figure 11.

I would like to thank Prof. G. W. Gray, FRS, Prof. S. T. Lagerwall and D. G. Porte for their reading of the manuscript and useful discussions suggesting several improvements. I also acknowledge D. B. Pech and Prof. J. E. Proust who introduced me to the study of two pharmaceutical drugs with remarkable liquid crystalline properties at the origin of this work on micelles and bilayers.

References

[1] (*a*) Winsor, P. A., 1948, *Trans. Faraday Soc*., **44,** 376; (*b*) Winsor, P. A., 1954, *Solvent Properties of Amphiphile Compounds* (London: Butterworth); (*c*) Winsor, P. A., 1968, *Chem. Rev*., **68,** 1; (*d*) Winsor, P. A., 1974, *Liquid Crystals and Plastic Crystals*, Vol. 1, edited by G. W. Gray and P. A. Winsor (Chichester: Ellis Horwood), pp. 199–287.

[2] Bourel, M., and Schechter, R. S., 1988, *Microemulsions and Related Systems, Formulation, Solvency and Physical Properties*, Surfactant Science Series, Vol. 30 (New York: Marcel Dekker, Inc.), p. 83.

[3] Tanford, C., 1973, *The Hydrophobic Effect* (New York: Wiley), p. 80.

[4] (*a*) Israelachvili, J. N., Mitchell, D. J., and Ninham, B. W., 1976, *J. Chem. Soc. Faraday Trans. 1*, **72,** 1525; (*b*) Israelachvili, J. N., 1991, *Intermolecular and Surface Forces*, 2nd Edn (New York: Academic Press).

[5] Petrov, A. G., and Bivas, I., 1984, *Prog. Surf. Sci*., **16,** 389.

[6] (*a*) Helfrich, W., 1981, *Physics of Defects*, Les Houches, session 35, edited by R. Balian, M. Kléman and J.-P. Poirier (Amsterdam: North Holland), pp. 716–755; (*b*) Helfrich, W., 1989, *Liq. Cryst*., **5,** 1647.

[7] Kleman, M., 1988, *Liq. Cryst*., **3,** 1355.

[8] (*a*) Bouligand, Y., 1990, *Geometry in Condensed Matter*, edited by J. F. Sadoc (World Scientific), pp. 193–231; (*b*) Bouligand, Y., 1990, *J. Physique*, **51,** C7–35; (*c*) Bouligand, Y., 1972, *J. Physique*, **33,** 525; (*d*) Bouligand, Y., 1980, *Dislocations in Solids*, edited by F. R. N. Nabarro (Amsterdam: North Holland), pp. 301–347.

[9] Helfrich, W., and Deuling, H. J., 1974, *J. Physique*, **36,** C1–327.

[10] Bingham, A. D., 1975, *Cell Membranes: Biochemistry, Cell Biology and Pathology*, edited by G. Weissman and R. Claiborne (New York Hospital Practice), pp. 24–34.

[11] Lipowski, R., 1991, *Nature*, **349,** 475.

[12] Sheetz, M. P., and Singer, S. J., 1974, *Proc. natl. Acad. Sci. USA*, **71,** 4457.

[13] Small, D. M., 1986, *Handbook of Lipid Research*, Vol. 4, edited by D. M. Small (New York and London: Plenum Press), pp. 43–87.

[14] Nageotte, J., 1937, *Morphologie des Gels Lipoïdes: Myéline, Cristaux Liquides, Vacuoles* (Paris: Hermann).

[15] Sekimura, T., and Hotani, H., 1991, *J. theor. Biol*., **149,** 325.

[16] Steinbrecht, R. A., 1968, in Proceedings of the 4th European Regional Conference on Electron Microscopy, Rome, Vol. 2, p. 221.

[17] (*a*) Johnson, B., and Talbot, P., 1987, *J. Crustacean Biol*., **7,** 288; (*b*) Talbot, P., and Zao, P., 1991, *J. Crustacean Biol*, **11,** 1.

[18] Weiss, L., 1983, *Cell and Tissue Biology, A Textbook of Histology*, 6th Edn (Baltimore, Munich: Urban & Schwarzengerg), pp. 790, 1060.

[19] Pech, B., Proust, J. E., Bouligand, Y., and Benoit, J. P., 1997, *Pharm. Res*., **14,** 37.

[20] Bouligand, Y., Boury, F., Devoisselle, J.-M., Fortune, R., Gautier, J.-C., Girard, D., Maillol, H., and Proust, J. E., 1998, *Langmuir*, **14,** 542.
[21] Bouligand, Y., Boury, F., Pech, B., Benoit, J. P., Gautier, J. C., and Proust, J. E., *Liq. Cryst*. (to be published).
[22] Charvolin, J., and Sadoc, J.-F., 1987, *J. Physique*, **48,** 1559.
[23] Scriven, L. E., 1977, in *Micellization, Solubilization and Microemulsions*, edited by K. L. Mittal (New York: Plenum), pp. 877–893.
[24] Luzzati, V., Delacroix, H., Gulik, A., Gulik-Krzywicki, T., Mariani, P., and Vargas, R., 1997, *Lipid Polymorphism and Membrane Properties*, edited by R. M. Epand (San Diego: Academic Press), Chap. 3.
[25] Porte, G., Appell, J., Bassereau, P., and Marignan, J., 1989, *J. Physique Fr*., **50,** 1335.
[26] Farago, B., Richter, D., Huang, J. S., Safran, S. A., and Milner, S. T., 1990, *Phys. Rev. Lett*., **65,** 3348.
[27] Meunier, J., and Lee, L. T., 1991, *Langmuir*, **7,** 1855.
[28] (*a*) Boltenhagen, P., Lavrentovich, O., and Kleman, M., 1991, *J. Physique II, Fr*., **1,** 1233; (*b*) Boltenhagen, P., Lavrentovich, O., and Kleman, M., 1992, *Phys. Rev. A*, **46,** 1743.
[29] Kellay, H., Meunier, J., and Binks, B. P., 1993, *Phys. Rev. Lett*., **70,** 1485.
[30] Klösgen, B., and Helfrich, W., 1997, *Biophys. J*., **73,** 3016.
[31] Chang, J. J., McDowall, A. W., Lepault, J., Freeman, R., Walter, C. A., and Dubochet, J., 1983, *Microscopy*, **132,** 109.
[32] Lin, Z., 1996, *Langmuir*, **12,** 1724.